*Journal of Orthopaedic Research*
**17**:532-539 The Journal of Bone and Joint Surgery, Inc.


# Quantitative Determination of Joint Incongruity and Pressure Distribution during Simulated Gait and Cartilage Thickness in the Human Hip Joint

R. von Eisenhart, C. Adam, *M. Steinlechner, M. Müller-Gerbl, and F. Eckstein

*Musculoskeletal Research Group, Anatomische Anstalt, Ludwig-Maximilians-Universität, München, and *Institut für Gerichtliche Medizin, Universität Innsbruck, Innsbruck, Germany*

**Summary:** The objective of this study was to provide quantitative data on hip-joint incongruity and pressure during a simulated walking cycle and on articular-cartilage thickness in the same set of specimens. Using a casting technique in eight specimens of the human hip (age: 18-75 years), we determined the width of the joint space (incongruity) required at minimal load for contact at four phases of the gait cycle. The pressure distribution, measured with pressure-sensitive film, was determined at physiologic load magnitudes on the basis of *in vivo* measurements of hip-joint forces. Cartilage thickness was assessed with A-mode ultrasound. At minimal loading, the average maximum width of the joint space ranged from 1.1 to 1.5 mm in the acetabular roof, with the contact areas located ventro-superiorly and dorso-inferiorly throughout the gait cycle. At physiological loading, the width decreased and the contact areas covered the complete articular surface during midstance and heel-off but not during heel-strike or toe-off. The pressure distribution was inhomogeneous during all phases, with average maximum pressures of 7.7 ± 1.95 MPa at midstance. The cartilage thickness varied considerably throughout the joint surfaces; maxima greater than 3 mm were found ventro-superiorly. These data can be used to generate and validate computer models to determine the load-sharing between the interstitial fluid and the solid proteoglycan-collagen matrix of articular cartilage, the latter being relevant for the initiation of mechanically induced cartilage degeneration.

Mechanical factors have been shown to play an important role in the initiation and progression of osteoarthritic cartilage changes (23,26,27), the normal function of the cartilage being to transmit forces from one body segment to another during static and dynamic loading. Articular cartilage is a multiphasic material; stresses are distributed in a time-dependent manner on its components, namely the proteoglycan-collagen matrix and the interstitial fluid (23). Because loads are shared between these two components, the relevant stresses within the cartilage cannot be measured but must be calculated (5).

Recent analytical solutions for the contact of two biphasic cartilage layers in idealized joints have suggested that hydrostatic pressurization of the fluid shields the proteoglycan-collagen matrix from as much as 90% of the load for the first 100-200 seconds of loading (5,6,35,36). The results depend on a number of other factors, including joint incongruity and cartilage thickness. The occurrence of hydrostatic pressure has also been confirmed in confined compression experiments (30). Because elastic (shear and tensile) stresses in the cartilage matrix (but not hydrostatic pressure in the interstitial fluid) are assumed responsible for mechanically induced cartilage degeneration, quantitative predictions of the load-sharing between the two phases are relevant for understanding the etiology of osteoarthritis in human joints.

Although physiological incongruity in the human hip joint has been recognized for some time (3,10, 19,28,29,32), calculation of hip-joint contact pressures has been based on the assumption that the cartilage surfaces make a perfect fit (8,11,18,21). No calculations have been presented for the time-dependent load-sharing between the proteoglycan-collagen matrix and fluid in the naturally incongruous hip joint. For this task, a nonlinear contact algorithm for biphasic soft tissues has been developed (12), and the amount of hydrostatic pressurization has been shown to depend not only on the degree, but also on the specific type, of joint incongruity (13). To allow quantitative predictions in the human hip joint, however, quantitative data regarding the specific incongruity and cartilage thickness are required. Such data have

Received September 15, 1998; accepted February 24, 1999.
Address correspondence and reprint requests to F. Eckstein at Anatomische Anstalt, Pettenkoferstrasse 11, D-80336 München, Germany. E-mail: eckstein@anat.med.uni-muenchen.de
Presented in part at the 44th annual meeting of the Orthopaedic Research Society, New Orleans, Louisiana, March 16-19, 1998.

**TABLE 1.** *Data for the midstance phase of gait*

| Specimen | Age (yr) | Joint space[a] (mm) | Contact area | Maximum pressure (MPa) | Acetabulum[b] (mm) | Femoral head[c] (mm) |
|---|---|---|---|---|---|---|
| 1 | 18 | 0.27 | Bicentric | 8.25 | 4.26 | 5.33 |
| 2 | 22 | 0.40 | Bicentric | 6.75 | 4.17 | 3.08 |
| 3 | 39 | 0.38 | Bicentric | 3.75 | 3.31 | 4.20 |
| 4 | 45 | 0.44 | Bicentric | 9.75 | 2.91 | 3.68 |
| 5 | 47 | 0.78 | Superior | 9.75 | | |
| 6 | 52 | 0.68 | Bicentric | 8.25 | 3.27 | 2.74 |
| 7 | 64 | 0.40 | Bicentric | 8.25 | 2.85 | 2.39 |
| 8 | 75 | 0.38 | Bicentric | 6.75 | 2.64 | 2.74 |

Joint-space width and contact areas were obtained at minimal load. Maximum contact pressure was obtained at physiological load. In one of the specimens, cartilage thickness could not be measured due to a technical problem. Bicentric = ventro-superior and dorso-inferior aspects of the acetabulum, and superior = acetabular roof.

[a] Average width of the joint space.

[b] Maximum cartilage thickness in the acetabulum.

[c] Maximum cartilage thickness in the femoral head.

been reported in a limited number of specimens (16) for the stance phase but not for other phases of the gait cycle.

The objective of the present study was to provide quantitative data for the design and validation of anatomically accurate computer models of the human hip joint at different phases of gait. In the same set of specimens, we determined (a) the anatomical width of the joint space (distance between cartilage layers) at the minimal load required for contact during heel-strike, midstance, heel-off, and toe-off; (b) the contact areas and pressure distribution for these phases, simulating physiological load magnitudes and directions (7); and (c) the cartilage thickness of the acetabulum and femoral head.

## MATERIALS AND METHODS

The experimental setup (load magnitude and direction during the gait cycle) was based on *in vivo* data by Bergmann et al. (7) on hip-joint loading during walking at a speed of 4 km/hour. A coordinate transformation of the femoral force data into a pelvic coordinate system (heel-strike, midstance [first force maximum], heel-off [second force maximum], and toe-off) has been previously performed on the basis of kinematic gait analysis (34).

Eight fresh cadaveric specimens of human hip joints without

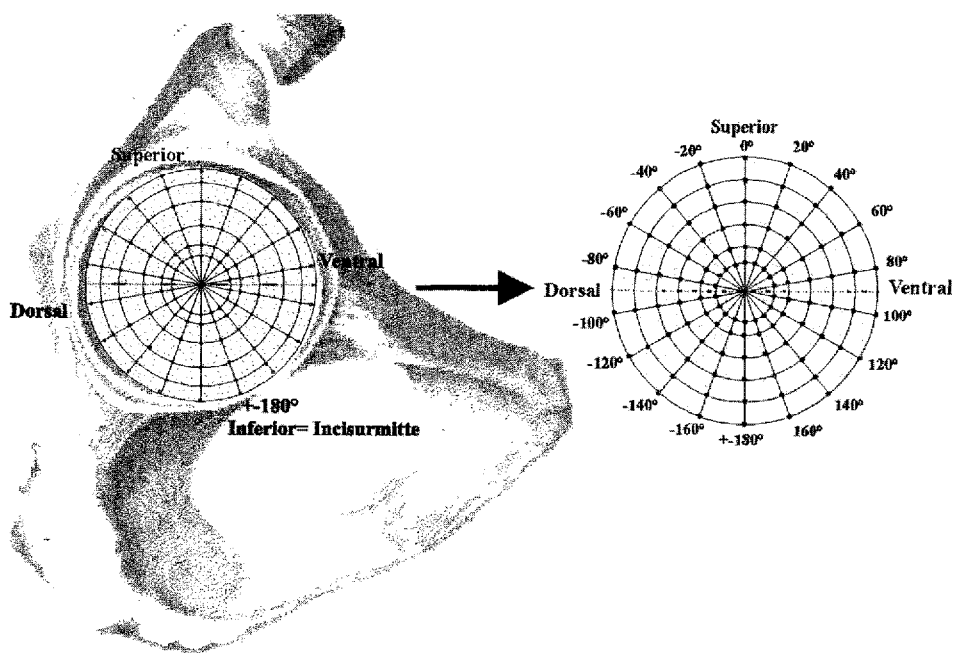


**FIG. 1.** Projectional grid for determining 108 measurement points of joint-space width and cartilage thickness throughout the acetabulum. The points are defined by six circles at 15° intervals (0-75° latitude, 0° = acetabular rim, and 90° = center of the acetabular fossa) and 18 meridians at 20° intervals (−180 and 180° = middle of the acetabular incisure, and 0° = acetabular roof).

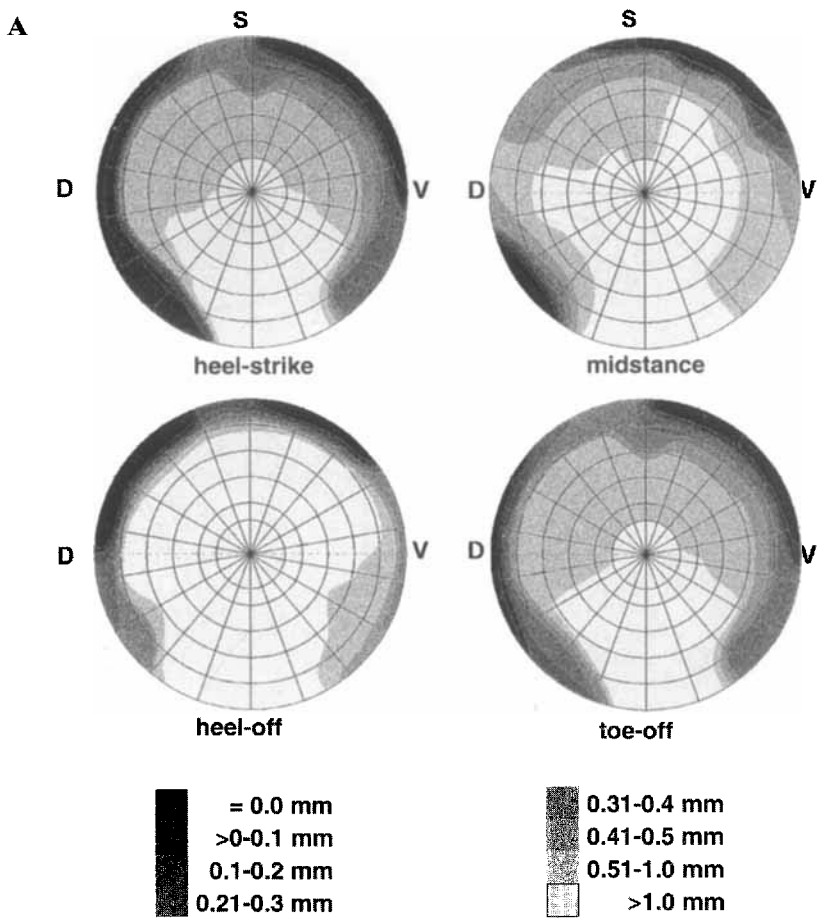


**FIG. 2.** Representative distribution of joint-space width (cast thickness) from one hip joint (specimen 6 in Table 1) at four instances of the walking cycle. (See Fig. 1 for orientation of the grid.) Thickness intervals of 0.1 mm are depicted by gray areas. At minimal load (**A**), there is contact at the ventro-superior and dorso-inferior aspects of the lunate surface and the width of the joint space increases toward the center of the surface. The distribution pattern varies little between the different phases of the walking cycle. At physiological loads (**B**), full contact is established during midstance and heel-off but not at heel-strike or toe-off. D = dorsal, V = ventral, and S = superior.

macroscopically visible cartilage lesions or other signs of musculoskeletal disease were obtained from eight individuals with a mean age of 45 years (range: 18-75 years, Table 1). Within 36 hours of death, the eight right hemipelves (sectioned at the middle of the sacrum and at the pubic symphysis) and the proximal part of the femur (sectioned 20 cm distal to the lesser trochanter) were removed. The specimens were stored at −20°C and thawed to room temperature before the investigation. The joint capsule was then opened and the joint was disarticulated, leaving the acetabular labrum intact. Joint cartilage was kept fully moist with Ringer's solution throughout the investigation.

The hemipelvis and femur were positioned in a materials testing machine (model 1445; Zwick, Ulm, Germany); the femur was mounted to the mobile element, and the hemipelvis was mounted to the testing table. The symphysis and sacrum were fixed to a wooden plate, and the iliac crest was supported from below. The hemipelvis rested on a mobile plate with one rotational and two translational degrees of freedom so that the constraining forces were minimized and free adjustment was allowed for the joint components; only very small forces (<1 N) were required for translation even under high loading pressures.

The joint components were mounted so that their relative positions corresponded with those during the four phases of the gait cycle (34), and the direction of load application corresponded with the direction of the joint reaction force measured *in vivo* (7). The direction (relative to the pelvis) and magnitude (for physiologic loading) of the load were as follows: (a) heel-strike: 94% body weight, sagittal angle 21° dorsal, and frontal angle 22° medial; (b) midstance (femur 5° before passing the vertical): 345% body weight, sagittal angle 5° ventral, and frontal angle 11° medial; (c) heel-off: 223% body weight, sagittal angle 14° dorsal, and frontal angle 12° medial; and (d) toe-off: 80% body weight, sagittal angle 7° ventral, and frontal angle 20° medial (34).

To determine joint incongruity (width of the joint space), a polyether casting material (Permadyne; ESPE, Seefeld, Germany) was placed in the acetabulum before application of the load (14-16). The fat pad below the transverse acetabular ligament was removed to allow the casting material to be displaced from the acetabulum during loading. Casts were obtained for the four phases of the gait cycle, first at the minimal load necessary for establishing contact between both joint components and then at physiological load magnitudes (7,34). For the eight loading configurations (four positions and two load magnitudes), the width of the joint space was determined at 108 points throughout the acetabulum. The points were defined by 18 meridians at 20° intervals (−180 and 180° = middle of the acetabular incisure, and 0° = acetabular roof) and six circles at 15° intervals (0-75° latitude, 0° = acetabular rim, and 90° = center of the acetabular fossa) (Fig. 1). The points were obtained, with the casts still in place, by projection of a grid perpendicular to the entrance plane of the acetabulum. The thickness of the casts was measured perpendicular to the femoral surface with a spherical distance sensor (IDS 543;

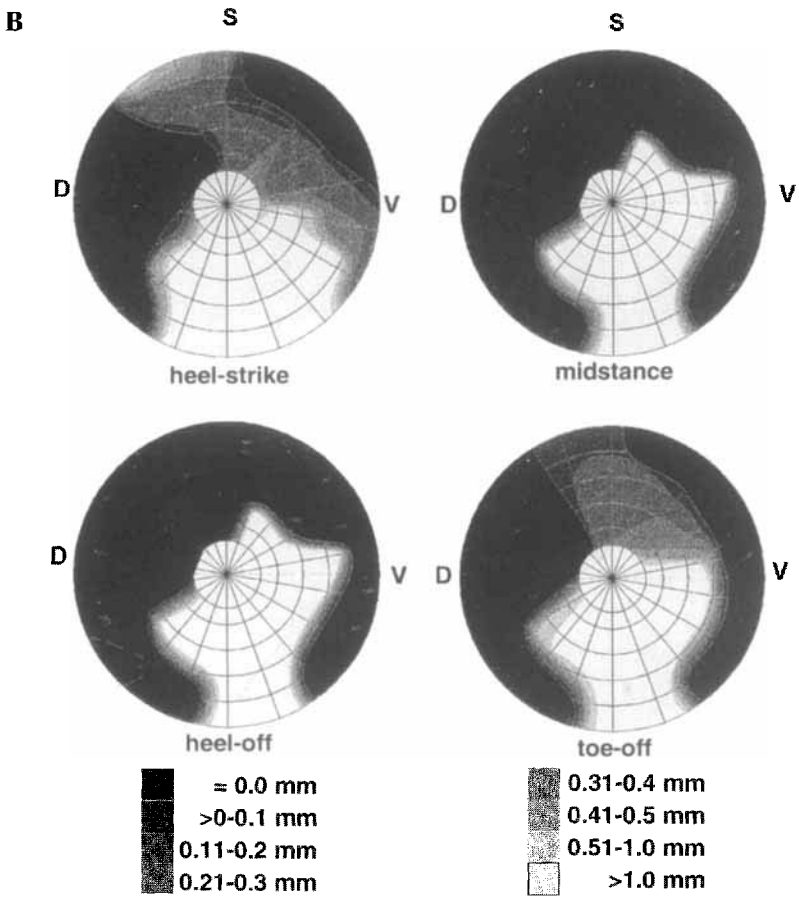


Mitutoyo, Neuss, Germany); the accuracy and reproducibility of this procedure was demonstrated previously (16). The mean width of the joint space in the acetabular roof (minimal loads) was calculated by averaging the values obtained at −40-40° (30 points).

Next, the pressure distribution in the acetabulum was determined with film of low sensitivity (2.5-10 MPa) (Prescale; Fuji, Tokyo, Japan). After the diameter of the femoral head was measured, the film was prepared for each specimen in form of a rosette with 12 petals to allow for a crinkle-free assessment (31). The film was sealed with thin polyethylene sheets, and physiological load magnitudes were applied at each position of the gait cycle corresponding to the *in vivo* measurements of Bergmann et al. (7). The stained films and a reference scale were digitized with an image analyzing system, and the color intensity was converted to pressure intervals of 1.5 MPa.

Cartilage thickness was measured with a previously validated A-mode ultrasound system (Digital Biometric Ruler 300; Sonometric Systems, Lüneburg, Germany) (2). To measure cast thickness, the grid with 108 points was projected on the acetabulum and the thickness was measured perpendicular to the cartilage surface at all points situated on the lunate surface. To determine the thickness of the corresponding femoral cartilage, the femur was placed in the acetabulum corresponding with its position at midstance and the acetabular rim was marked on the femoral head. From all values measured on each surface, we determined the maximum and mean thickness of the acetabular and femoral cartilage. Inhomogeneity of cartilage thickness was quantified by calculating the coefficient of variation (CV% = SD/mean) for all 108 thickness values for each surface (2,4).

Quantitative differences between parameters were tested for statistical significance with use of the Wilcoxon signed-rank test for matched pairs (Statview 4.5; Abacus Concepts, Berkely, CA, U.S.A.).

## RESULTS

At minimal load, the width of the joint space always increased from the acetabular margin toward the central aspects of the acetabulum. In seven of the eight joints, a bicentric contact pattern was recorded, with contact areas at the ventro-superior and dorso-inferior aspects of the lunate surface and no contact at major parts of the acetabular roof (Fig. 2A). These bicentric patterns generally varied only slightly between the four phases of the walking cycle. In the acetabular roof of these seven specimens (30 measuring points from −40 to 40°), the average maximum thickness of the cast was 1.32 ± 0.25 mm (mean ± SD) at heel-strike, 1.46 ± 0.40 mm at midstance (first maximum), 1.10 ± 0.52 mm at heel-off (second maximum), and 1.11 ± 0.45 mm at toe-off, with no statistical differences between these phases. The mean width of the joint space in the acetabular roof was 0.63 ± 0.18 mm at heel-strike, 0.45 ± 0.17 mm at midstance, 0.45 ± 0.26 mm at heel-off, and 0.46 ± 0.29 mm at toe-off. The mean width of the joint space in the acetabular roof was significantly higher at heel-strike than at midstance or heel-off ($p < 0.05$), but there were no significant differences between the other phases. In one specimen, almost the entire

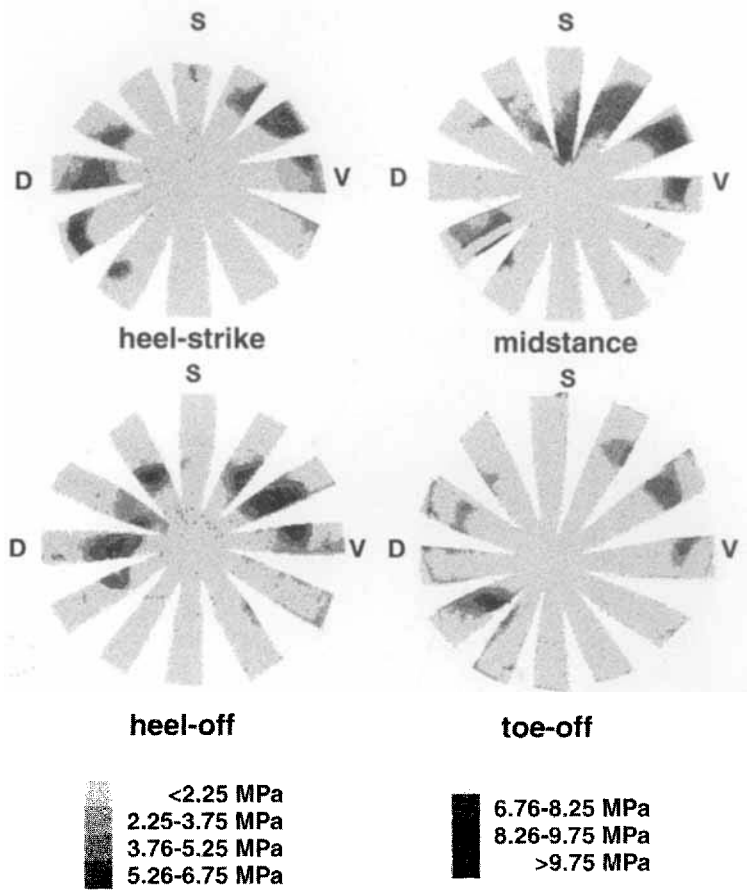


**FIG. 3.** Pressure distribution throughout the lunate surface of the specimen in Fig. 2 at physiological load magnitudes. Maximum pressure is observed at the ventro-superior and dorso-inferior aspects. The gray areas indicate intervals of 1.5 MPa. D = dorsal, V = ventral, and S = superior.

acetabular roof was in contact at minimal loads during the four phases of gait (Table 1). The width of the joint space in the anterior and posterior horns of the lunate surface was substantially higher in that specimen than in the other seven specimens.

At physiological load magnitudes, four joints had contact throughout the lunate surface during midstance and heel-off but only partial contact during heel-strike and toe-off (Fig. 2B). In the other four joints, the entire lunate surface was in contact with the femoral head during the four phases of gait.

The maximum pressure recorded in the acetabulum was 6.4 ± 1.75 MPa at heel-strike, 7.7 ± 1.95 MPa at midstance, 6.4 ± 1.33 MPa at heel-off, and 5.4 ± 1.7

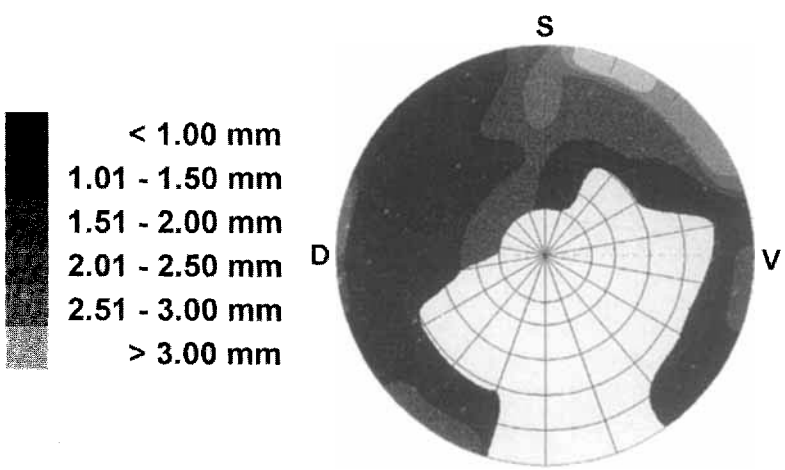


**FIG. 4.** Distribution of cartilage thickness throughout the lunate surface of the specimen in Fig. 2. The cartilage thickness was considerably inhomogeneous. Maximum cartilage thickness was recorded at the ventro-superior aspect of the acetabulum. Cartilage thickness values are depicted in intervals of 0.50 mm. D = dorsal, V = ventral, and S = superior.

MPa at toe-off. The highest value was 9.75 MPa and occurred during midstance (Table 1). The values were significantly higher at midstance than at heel-strike or toe-off ($p < 0.05$), with no significant differences between the other phases. The high variation in the loading forces during the four phases of the gait cycle was not reflected by a proportional variation in the maximum pressure.

At lower magnitudes of load (heel-strike and toe-off), the load-bearing areas were located at the acetabular margin, whereas at higher loads (midstance and heel-off) they shifted toward the more central parts of the lunate surface (Fig. 3). All specimens had a pressure peak in the ventro-superior part of the lunate surface during the four phases. An additional maximum was recorded in five joints in the dorso-inferior aspect of the lunate surface during the four phases, as well as in two specimens during one further position of the gait cycle (heel-strike or heel-off). The locations of the load-bearing areas at physiological load magnitudes were generally in agreement with the contact areas observed at minimal load (Figs. 2 and 3).

Maximum cartilage thickness was found ventro-superiorly in the acetabulum (Fig. 4) and in the femoral head. The location of maximum thickness agreed with the ventro-superior location of maximum pressure recorded during the four phases of the walking cycle; the thickness ranged from 2.6 to 4.3 mm in the acetabulum (average = 3.3 mm) and from 2.4 to 5.3 mm in the femoral head (average = 3.5 mm). In general, cartilage thickness decreased with age (Table 1). There was no statistical difference between the values for maximum thickness on both surfaces, although the mean thickness of the femoral cartilage (1.5-2.0 mm, average: 1.7 mm) was higher ($p < 0.01$) than that of the acetabulum (1.1-1.7 mm, average: 1.4 mm). The coefficient of variation of the thickness distribution ranged from 24 to 48% (mean: 36%) in the femoral head and from 31 to 49% (mean: 38%) in the acetabulum, suggesting an inhomogeneous cartilage thickness in both surfaces.

## DISCUSSION

This is the first study, to our knowledge, to provide quantitative data on natural hip-joint incongruity and pressure distribution during a simulated walking cycle and on articular-cartilage thickness in the same specimens. These data are required for the design and validation of anatomically accurate computer models of the human hip joint that aim to calculate the load-sharing between the interstitial fluid and solid proteoglycan-collagen matrix of articular cartilage. At minimal load, an important joint-space width was observed in the acetabular roof, increasing from the acetabular rim to the central aspects of the lunate surface. Although the distribution of the width varied between individuals, its distribution at four phases of the walking cycle was remarkably constant in each individual. The pressure distribution was highly inhomogeneous, and maximum contact stresses were recorded in the ventro-superior aspect of the lunate surface during midstance. The cartilage thickness was highly variable in the acetabulum and femoral head, with maxima greater than 3 mm located ventro-superiorly.

The loading configuration applied in this study was based on *in vivo* measurement, with a telemetric endoprosthesis (7), of hip-joint forces at a walking speed of 4 km/hour. These data were recorded from only one patient, whose muscular coordination and walking pattern may be different from that of a young healthy person. However, the measurements were performed 30 months after surgery, so that the patient had regained a relatively normal walking pattern (7). These data do not rely on assumptions about neuromuscular control mechanisms and therefore have the advantage over theoretical calculations. For the experimental setup, the direction of the loading forces was converted to a pelvic coordinate system on the basis of kinematic gait analysis (34). The direction of the reaction force of the joint with respect to the acetabular entrance plane was relatively constant throughout gait (34).

For modeling purposes, quantitative data on the initial incongruity of the hip (without deformation of the cartilage) are required. We therefore used the minimal load needed to displace the casting material and establish contact between the acetabulum and femoral head. To avoid sealing of the cast in the acetabulum, the fat pad below the transverse acetabular ligament was removed so that the material could displace with minimal resistance by way of the acetabular fossa. For measurements at minimal load, we expected no deformation in the pelvic bone; at physiologic load magnitudes, however, the pelvic ring was likely to deform. The hemipelvis was fixed at the symphysis, sacrum, and iliac crest; although the hemipelvis can deform in this setup, the fixation did not entirely correspond with the physiological situation in which the forces are balanced by a multitude of muscle attachments. The normal deformation of the acetabulum with simulation of muscular attachment has been shown, however, to range from only 10 to 60 μm during walking (24). Because the incongruity recorded in our study is at least one order of magnitude higher than the acetabular deformation, we do not expect that this deformation had a major effect on load transmission in the hip-joint surfaces. This is confirmed by the agreement of our results with those of Widmer et al. (33), who, using an entire pelvis and simulating muscular attachments without fixation of the pubic symphysis, measured pressure distribution during single-leg stance.

The use of pressure-sensitive film is a limitation of

our study because the film thickness of 200 μm can cause potential distortions of the true shape of the articular surfaces. The location of the load-bearing areas recorded with the Fuji film was, however, very similar to that of the contact areas, obtained with the casting material, at which no such geometric distortion occurred.

The current study extends our earlier findings on hip-joint incongruity during the stance phase of gait (16) by showing that the distribution of joint-space width is relatively constant during the gait cycle. This suggests that the parts of the femoral surface that make contact during gait can be approximated by a sphere, whereas the acetabulum deviates from a perfect fit with the femoral cartilage. This is in agreement with the finding of Bullough et al. (10) of the relatively high degree of asphericity of the acetabulum. In accordance with Afoke et al. (3), we observed some differences in the width of the joint space between individuals. Contrary to our previous study in which older specimens were investigated, the predominant contact pattern was bicentric, with contact taking place ventro-superiorly and dorso-inferiorly in the acetabulum. It should be noted that in our previous study, a walking speed of 2 (rather than 4) km/hour was simulated (16) (the reaction force of the joint taking a more ventral course at the higher walking speeds [7]) and only two fresh specimens were investigated (the others had been embalmed with 4% formalin).

The location of the load-bearing areas recorded with Fuji film was relatively constant throughout gait, although the areas had a slightly more peripheral location for lower load magnitudes (heel-strike and toe-off) and shifted toward the central aspects of the lunate surface at higher forces (midstance and heel-off). This can be explained by the fact that the anterior and posterior horns of the lunate surface spread apart as the femoral head presses into the acetabulum. Using a hemispherical device with pressure instrumentation, Rushfeldt et al. (28,29) reported a bicentric distribution of contact stress and maximum pressures of about 5.5 MPa for loads of 250% body weight. The peak pressures in our study do not scale linearly with the applied reaction forces of the joint. This may be explained by the increase in load-bearing areas at higher forces. Although the pressure patterns are clearly influenced by the individual joint incongruity, we cannot rule out that the inhomogeneous support of the subchondral acetabular bone (11,33) may also play an important role in the distribution of acetabular contact stress.

The cartilage of the hip has been shown to yield a highly inhomogeneous thickness distribution, the inhomogeneity being in the same range as that of the knee (1,4). The maximum cartilage thickness was always found in the periphery of the ventral aspect of the acetabular roof, in agreement with previous studies (1,25) and equivalent to the site of maximum contact pressure found in our current analysis. This supports the hypothesis that the distribution of cartilage thickness is related to the distribution of the long-term stress acting on the joint surfaces (25). The results, however, contrast somewhat with those of Rushfeldt et al. (28,29), who described maximum thickness in the peripheral part of the posterior horn of the lunate surface. Compared with findings in older individuals (1), the mean and, in particular, maximum thickness values were higher in our study. Due to the highly inhomogeneous thickness of both cartilage layers, the incongruity of the hip joint cannot be accurately estimated from radiographs or computed tomography scans. Calculations of the pressure distribution in the hip joint that are based on these types of imaging modalities (9,20,22) therefore suffer important limitations.

To design a finite-element model from these data, the absolute shape of at least one surface must be known. The uniform distribution of the contact areas during different phases of the walking cycle suggest that the femoral head may be approximated as a sphere. Starting with this surface, the cartilage surface of the acetabulum can be constructed from our data on relative incongruity, and the shape of the bone-cartilage interfaces of the femoral head and acetabulum can be constructed from our results on cartilage thickness. The relative difference in shape between the acetabular and femoral surfaces (as measured in this study) has a much more profound effect on the stress acting on and within the cartilage than does a small deviation of the femoral shape from a perfect sphere. The contact areas and pressure distribution obtained for physiological load magnitudes can then be used to validate the results of a finite-element analysis.

If appropriate material properties are assigned to the cartilage and bone, and if adequate nonlinear contact algorithms for biphasic material are applied (12), the geometric data from our study allow calculation of the load-sharing between the interstitial fluid and solid proteoglycan-collagen matrix of articular cartilage. Joint incongruity and cartilage thickness have been shown to affect the load-sharing between the fluid and solid cartilage phases in theoretical calculations and in idealized joint models (5,6,13,35,36); therefore, numerical calculations based on accurate anatomic relationships may provide important insight into the mechanical pathogenesis of osteoarthritic changes. With the advent of magnetic resonance imaging, it should also become feasible to noninvasively determine cartilage thickness (17) and asphericity in the hip and to relate variations of joint incongruity between individuals to the individual propensity to

develop cartilage damage. Application of nonlinear contact algorithms (12) and implementation of variations in joint incongruity and cartilage thickness may thus bring about a closer agreement between the predictions of cartilage stresses in hip models and patient outcome in clinical studies (9,22).

**Acknowledgment:** We would like to thank Johannes Landgraf for his help with the experimental setup. Some of the data presented in this study were obtained as part (in preparation) of the doctoral thesis of Rüdiger von Eisenhart-Rothe at the Ludwig-Maximilians-Universität, München.

## REFERENCES

1. Adam C, Eckstein F, Milz S, Putz R: The distribution of cartilage thickness within the joints of the lower limb of elderly individuals. *J Anat* 193:203-214, 1998
2. Adam C, Eckstein F, Milz S, Schulte E, Becker C, Putz R: The distribution of cartilage thickness in the knee joint of old-aged individuals: measurement by A-mode ultrasound. *Clin Biomech* 13:1-10, 1998
3. Afoke NYP, Byers PD, Hutton WC: The incongruous hip joint: a casting study. *J Bone Joint Surg [Br]* 62:511-514, 1980
4. Ateshian GA, Soslowsky LJ, Mow VC: Quantitation of articular surface topography and cartilage thickness in knee joint using stereophotogrammetry. *J Biomech* 24:761-776, 1991
5. Ateshian GA, Lai WM, Zhu WB, Mow VC: An asymptotic solution for the contact of two biphasic layers. *J Biomech* 27:1347-1360, 1994
6. Ateshian GA, Wang H: A theoretical solution for the frictionless rolling contact of cylindrical biphasic articular cartilage layers. *J Biomech* 28:1341-1355, 1995
7. Bergmann G, Graichen F, Rohlmann A: Hip joint loading during walking and running, measured in two patients. *J Biomech* 26:969-990, 1993
8. Brand R, Miller J, Andrews J: Quantifying osteoarthrotic hip incongruency: an approach to optimizing osteotomies. *Trans Eur Orthop Res Soc* 7:314, 1997
9. Brinckmann P, Frobin W, Hierholzer E: Stress on the articular surface of the hip joint in healthy adults and persons with idiopathic osteoarthrosis of the hip joint. *J Biomech* 14:149-156, 1981
10. Bullough PG, Goodfellow J, Greenwald AS, O'Connor J: Incongruent surfaces in the human hip joint. *Nature* 217:1290, 1968
11. Dalstra M, Huiskes R: Load transfer across the pelvic bone. *J Biomech* 28:715-724, 1995
12. Donzelli P, Spilker RL: A contact finite element formulation for biological soft hydrated tissues. *Comput Methods Appl Mech Eng* 153:68-79, 1998
13. Donzelli PS, Eckstein F, Putz R, Spilker RL: Physiological joint incongruity significantly affects the load partitioning between the solid and fluid phases of articular cartilage. *Trans Orthop Res Soc* 22:82, 1997
14. Eckstein F, Löhe F, Schulte E, Müller-Gerbl M, Milz S, Putz R: Physiological incongruity of the humero-ulnar joint: a functional principle of optimized stress distribution acting upon articulating surfaces? *Anat Embryol* 188:449-455, 1993
15. Eckstein F, Löhe F, Hillebrand S, Bergmann M, Schulte E, Milz S, Putz R: Morphomechanics of the humero-ulnar joint. I. Joint space width and contact areas as a function of load and flexion angle. *Anat Rec* 243:318-326, 1995
16. Eckstein F, von Eisenhart-Rothe R, Landgraf J, Adam C, Loehe F, Müller-Gerbl M, Putz R: Quantitative analysis of incongruity, contact areas and cartilage thickness in the human hip joint. *Acta Anat* 158:192-204, 1997
17. Eckstein F, Schnier M, Haubner M, Priebsch J, Glaser C, Englmeier K-H, Reiser M: Accuracy of cartilage volume and thickness measurements with magnetic resonance imaging. *Clin Orthop* 352:137-148, 1998
18. Ferguson SJ, Bryant JT, Ito K: An investigation of the functional role of the acetabular labrum using a poroelastic fe-model. *Trans Orthop Res Soc* 8:92, 1998
19. Greenwald AS, O'Connor JJ: The transmission of load through the human hip joint. *J Biomech* 4:507-528, 1971
20. Hipp JA, Sugano N, Noble PC, Murphy SB: Relationship between peak pressures, mean pressures, contact areas and loading in the hip joint. *Trans Orthop Res Soc* 23:196, 1998
21. Macirowski T, Tepic S, Mann RW: Cartilage stresses in the human hip joint. *J Biomech Eng* 116:10-18, 1994
22. Maxian TA, Brown TD, Weinstein SL: Chronic stress tolerance levels for human articular cartilage: two nonuniform contact models applied to long-term follow-up of CDH. *J Biomech* 28:159-166, 1995
23. Mow VC, Ratcliffe A: Structure and function of articular cartilage and meniscus. In: *Basic Orthopaedic Biomechanics*, 2nd ed, pp 113-177. Ed by VC Mow and WC Hayes. Philadelphia, Lippincott-Raven, 1997
24. Noble PC, Paul JP: The deformation of the acetabulum during walking. *Trans Orthop Res Soc* 20:709, 1995
25. Oberländer W: [The stress of the human hip joint. VII. The distribution of cartilage thickness in the acetabulum and its functional explanation]. *Anat Embryol* 150:141-153, 1977
26. Radin EL, Rose RM: Role of subchondral bone in the initiation and progression of cartilage damage. *Clin Orthop* 213:34-40, 1986
27. Radin EL, Burr DB, Caterson B, Fyhrie D, Brown TD, Boyd RD: Mechanical determinants of osteoarthrosis. *Semin Arthritis Rheum* 21(3 Suppl 2):12-21, 1991
28. Rushfeld PD, Mann RW, Harris WH: Influence of cartilage geometry on the pressure distribution in the human hip joint. *Science* 204:413-415, 1979
29. Rushfeldt PD, Mann RW, Harris WH: Improved techniques for measuring in vitro the geometry and pressure distribution in the human acetabulum. I. Ultrasonic measurement of acetabular surfaces, sphericity and cartilage thickness. *J Biomech* 14:253-260, 1981
30. Soltz MA, Ateshian GA: Experimental verification of cartilage fluid pressurization in confined compression creep and stress relaxation. *Trans Orthop Res Soc* 23:224, 1998
31. von Eisenhart-Rothe R, Eckstein F, Müller-Gerbl M, Landgraf J, Rock C, Putz R: Direct comparison of contact areas, contact stress and subchondral mineralization in human hip joint specimens. *Anat Embryol* 195:279-288, 1997
32. Walmsley T: The articular mechanics of the diarthroses. *J Bone Joint Surg* 10:40-45, 1928
33. Widmer KB, Zurfluh B, Morscher EW: [Contact surface and pressure load at implant-bone interface in press-fit cups compared to natural hip joints]. *Orthopäde* 26:181-189, 1997
34. Witte H, Eckstein F, Recknagel S: A calculation of the forces acting on the human acetabulum during walking: based on in vivo force measurements, kinematic analysis and morphometry. *Acta Anat* 160:269-280, 1997
35. Wu JZ, Herzog W, Ronsky J: Modeling axi-symmetrical joint contact with biphasic cartilage layers: an asymptotic solution. *J Biomech* 29:1263-1281, 1996
36. Wu JZ, Herzog W, Epstein M: An improved solution for the contact of two biphasic cartilage layers. *J Biomech* 30:371-375, 1997